[12,26,33]. Concentrations below 5nM cannot be reliably sensed since the detected photocurrent values vary due to changes in backscattered excitation light. Small perturbations in the position of the well containing the dye relative to the sensor as well as the laser output power fluctuations cause variations in the detected control signal on the order of 1 pA-RMS. However, within a measurement, the noise floor is measured to be 0.25 pA-RMS, equal to
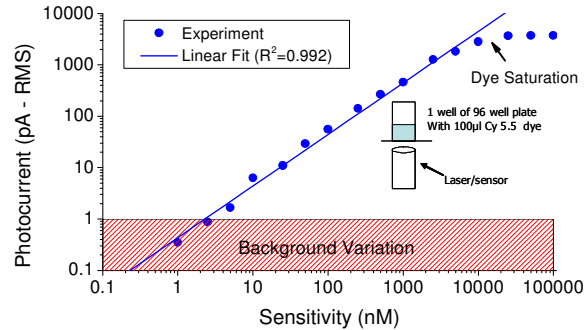

Fig. 5. Measured response of the integrated sensor to varying concentrations of Cy5.5 in PBS solution; Inset: schematic of the experiment

three standard deviations (3σ) of the mean signal sensed during the control measurements (N = 10). This implies that this sensor could likely detect Cy5.5 concentrations as low as 1nM using a better-controlled sample volume, such as in a microfluidic system. We note that the sensitivity, measured as a concentration (moles/liter) is strongly dependent on the volume illuminated by the VCSEL excitation source, and the sensor collection efficiency from that volume into the detector. A detailed quantitative analysis of these factors is described in our previous work [12,26]. We specifically targeted a large interrogation volume for in vivo tissue measurements. Greater sensitivity could be achieved by optimizing the collection efficiency of the detector to interrogate a much smaller volume. For our sensing geometry, the illuminated volume in the dye well is determined by the beam width of the VCSEL after the collimation lens (~2mm) and the dye depth (~3mm). This results in an excited dye solution volume of ~10µL, or 50 femtomole of excited dye molecules at the lowest measured sensitivity (5nM). To the best of our knowledge, this concentration sensitivity is comparable to the highest performing integrated fluorescence sensors at other wavelengths [27].

5.2 In vivo sensitivity

The sensitivity of the integrated sensor to in vivo fluorophore is determined by measuring fluorescence emission from subcutaneous injections of Cy5.5 dilutions in the dorsum of live, anesthetized, nude (Nu/Nu) mice. All animal studies were approved by the Institutional Administrative Panel on Laboratory Animal Care. Each mouse is anesthetized using 2-3% isofluorane, and we utilize two sensors in contact with the future injection sites on the left and right dorsum of the mouse to record a background measurement (Fig. 6a). The mouse then receives a 50µL subcutaneous injection of a Cy5.5 dilution in the right dorsum. The left dorsum is used as a control, with either no injection, or with an injection of buffer solution. The experiment is repeated for varying concentrations, with each concentration measured for at least 2 trials in different mice. Similar to the in vitro experiment, the fluorescence signal is determined by subtracting the background signal (due to backscattering and autofluorescence) from the measured photocurrent after injection. After measuring with the integrated sensor, the mouse is brought to a small animal CCD-based fluorescence imager (IVIS, Caliper Life Sciences, Hopkinton, MA) for comparison. We have verified using time sequential imaging that the detected fluorescence intensity does not change appreciably in the time elapsed between the sensor measurements and CCD imaging steps.

Figure 6b displays the response of the integrated sensor to the varying concentrations of subcutaneously injected Cy5.5 solution. The response is linear over two orders of magnitude,

with a detection limit of approximately 50nM. Similar to the discussion above for the in vitro sensitivity, and assuming a tissue penetration depth of ~2mm [26], a concentration of 50nM corresponds to 320 femtomole Cy5.5 dye molecules in the interrogated volume. Minimum detection in vivo is also limited by uncertainty due to background variation. For example, while collecting background data before injection, placement of the sensor in several locations around the control site causes the signal to vary by approximately 3pA-RMS. This higher variability, compared to the in vitro measurement, may be due to both variations in autofluorescence and excitation backscatter. The measurement is validated by comparing the sensor photocurrent to data collected with a CCD-based small animal imaging system. Figure 7a shows the maximum radiance observed from a region of interest enclosing the injection site plotted against the integrated sensor photocurrent. There is excellent correlation over the entire range of Cy5.5 concentrations, validating the performance of the miniature sensor. Figure 7b shows fluorescence images of two animals which have been separately injected with 25nM and 50nM Cy5.5 solutions, collected with a CCD-based small animal imaging system. The image of the 50nM animal shows a maximum radiance at the injection site approximately two times higher than the autofluorescence in the remainder of the animal. There is no contrast between the autofluorescence from the 25nM injection site and other sections of the mouse. The data shows that 675nm nude mouse autofluorescence in the Cy5.5 emission band is at the same magnitude as 25-50nM subcutaneous concentrations of Cy5.5.
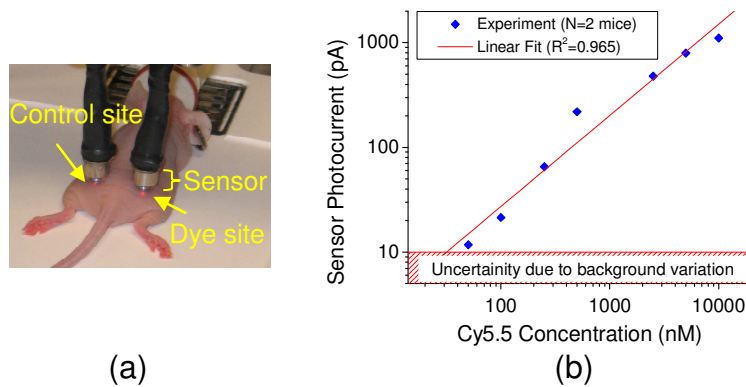

Fig. 6. (a) Photograph showing the sensor placement during an experiment in a living mouse to determine sensitivity and (b) experimental response of the sensor to varying concentrations of subcutaneously injected Cy5.5 in nude mice (N = 2 mice at each concentration)
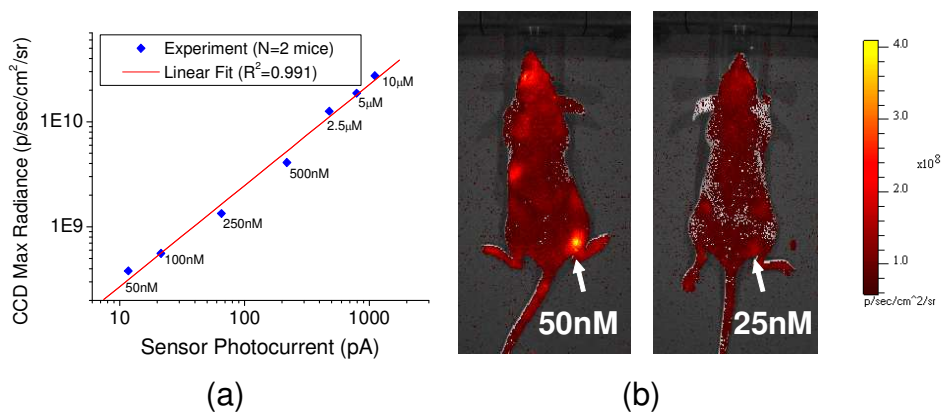

Fig. 7. (a) Comparison of the integrated sensor response to data from a CCD-based small animal fluorescence imager and (b) fluorescence images of mice injected with 50 and 25nM concentrations of Cy5.5

This agrees well with the 50nM autofluorescence limit reported by Sevick-Muraca and Rasmussen [25]. Importantly, we show that the integrated fluorescence sensor device is not limited by technological constraints, but instead by the autofluorescence of the animal subject in this application. Furthermore, this miniature sensor is designed to enable long-term interrogation of deep tissue by directly implanting it in close proximity to the target. Such a sensor provides the level of sensitivity as the large-format CCD-based fluorescence imagers utilized in numerous applications while providing better temporal resolution and opportunity for long-term continuous recording of fluorescence from freely-moving living subjects.

6. Conclusion

We have designed and fabricated an implantable, semiconductor-based sensor for in vivo fluorescence sensing in small animals. Similar to devices developed for lab-on-a-chip applications, the sensor is a monolithic integration of the optical components of a fluorescence imager, including a laser source, photodetector, and fluorescence emission filter. We have extended the sensor technology into far-red/visible wavelengths, which enables a commonly-used class of fluorescent probes and emerging fluorescent proteins, and discussed our design choices that optimize the device for sensing in living small animals. The sensor is sensitive to 5nM Cy5.5 in vitro and 50nM in nude mice, limited in vivo by the autofluorescence from the animal tissue, and not by the sensor technology. This miniature sensor thus provides the same sensitivity as large-format fluorescence imagers in this wavelength range. These sensors are promising to provide continuous, real-time molecular sensing that can enhance the basic understanding of molecular processes including tumor growth and drug treatment response all in live animals.

Future work includes implanting the sensor inside a live animal in order to evaluate stability and performance of the device over time periods from several hours to days. We also plan to further miniaturize the sensor package in order to make it less invasive to the animal. Since the present device relies on the electronic readout of a low-level current signal, we are in the process of incorporating components to amplify the sensor signal and thus reduce electrical noise. When completed, we hope to demonstrate real-time, continuous fluorescence sensing in freely-moving rodents.